THE AMERICAN MINERALOGIST, VOL. 51, MAY–JUNE, 1966

WEATHERING EFFECTS ON THE STRUCTURES OF MICA-TYPE CLAY MINERALS

NECIP GÜVEN[1] AND PAUL F. KERR,
Columbia University, New York, N. Y.

ABSTRACT

Mica-type clay minerals have been subjected to intensive weathering in the basin of the Willard Reservoir, north of Ogden near the margin of Great Salt Lake. Weathering attacks the interlayer portion of the structure of layer silicates most intensively where the bonds are weakest. A continuous scattering in the lower angle region of the (00*l*) reflection shows a random insertion of different groups of atoms between the mica-type layers.

The pronounced continuous scattering accompanying the (02, 11) diffraction band on the Guinier photographs and the absence of (*hkl*) reflections show that the layer silicates in the Willard clays possess an intensive disorder in their stacking sequence. The values of the *b* dimensions, high SiO_2/Al_2O_3 ratios, and appreciable amounts of $MgO+FeO+Fe_2O_3$ indicate that the mica-type layers before weathering were similar to tetrasilicic members of dioctahedral micas.

INTRODUCTION

The playas of the Great Basin are the relict floors of Quaternary pluvial lakes. Their argillaceous sediments have a high saline content and undergo intensive alteration owing to repeated desiccation and flooding and to other agents of weathering.

The Willard Reservoir (Fig. 1), on the flat northeast margin of Great Salt Lake is enclosed except on the northeast by a wide, low man-made dike, and furnishes an example of a repeatedly saturated playa clay. Prior to reservoir construction the area was intermittently flooded with saline lake water. The material for the dike was excavated from the clay floor to form a broad low dike and left to dry. The clay floor of the reservoir consists of partly dried clay materials which form a compact mass coated with precipitated saline minerals. The bluish clay in the borrow pits, however, during the 5 year construction interval was still in contact with saline reservoir water. Two groups of samples have been studied in the laboratory, one collected from the clay borrow pits, the other from the floor between the clay borrow pits. The former are referred to as "blue clays" and the latter as "saliniferous clays."

Weathering features of the layer silicates have been examined, but no attempt has been made to distinguish between post- and pre-depositional weathering. A brief description is also given of the saline minerals and the particle size distribution of the samples.

[1] Present address: Geophysical Laboratory, Carnegie Institution of Washington, Washington, D. C.

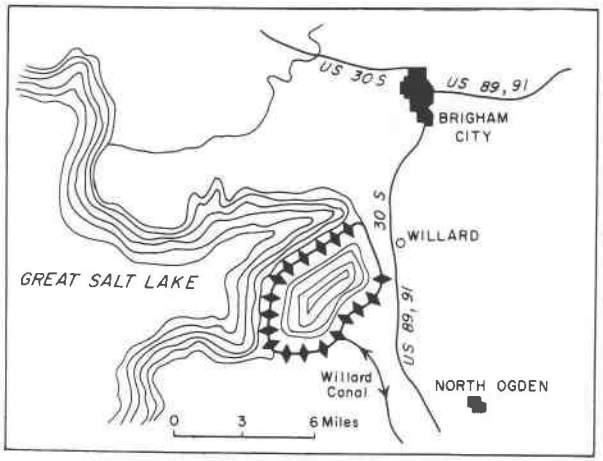

FIG. 1. Location of Willard Reservoir, along northeast shore of Great Salt Lake, Utah.

SALINES AND PARTICLE SIZE DISTRIBUTION

Salines. *X*-ray diffraction data show that the principal salines are halite, gypsum, calcite, and dolomite; minor amounts of sylvite and thenardite are also present. Relative amounts of the saline minerals in the samples studied are given in Table 1, as calculated from chemical analyses.

Particle size distribution. Figure 2 gives curves for the particle size distribution in the Willard clays, obtained by the A.S.T.M. hydrometer method D422.61T (A.S.T.M. Standards, 1961, p. 1272). The samples have few particles with a diameter greater than 100 microns. The proportion of colloidal particles is much lower in the saliniferous clays than

TABLE 1. THE DISTRIBUTION (PER CENT) OF SALINE MINERALS BASED ON CHEMICAL ANALYSES[1] OF REPRESENTATIVE SAMPLES

Sample	Halite	Gypsum	Calcite	Dolomite	Sylvite	Thenardite	Total
Blue clay No. 1	5.93	1.00	4.69	1.75	—	—	13.37
Saliniferous clay No. 2	3.06	13.58	11.51	—	[2]	—	28.15
Saliniferous clay No. 4	6.66	13.28	6.69	—	—	[2]	26.63

[1] Analyst, Silve Kallman, Ledoux and Company, Inc., New Jersey.

[2] Detected by *x*-rays, but not calculated from the chemical analyses of the anions, as all Cl^- is included in NaCl and all $SO_4^=$ in gypsum.

in the blue clays. In the former about 35–61 per cent have equivalent diameters less than 2 microns.

X-RAY DIFFRACTION OF THE WILLARD CLAY MINERALS

Clay mineral concepts. Mica-type clay minerals—illite, vermiculite, and montmorillonite—may be regarded as "disordered mica-type structures" which gain, with decreasing grain size, the electrochemical properties of colloidal particles. The most sensitive region of the layer silicate struc-

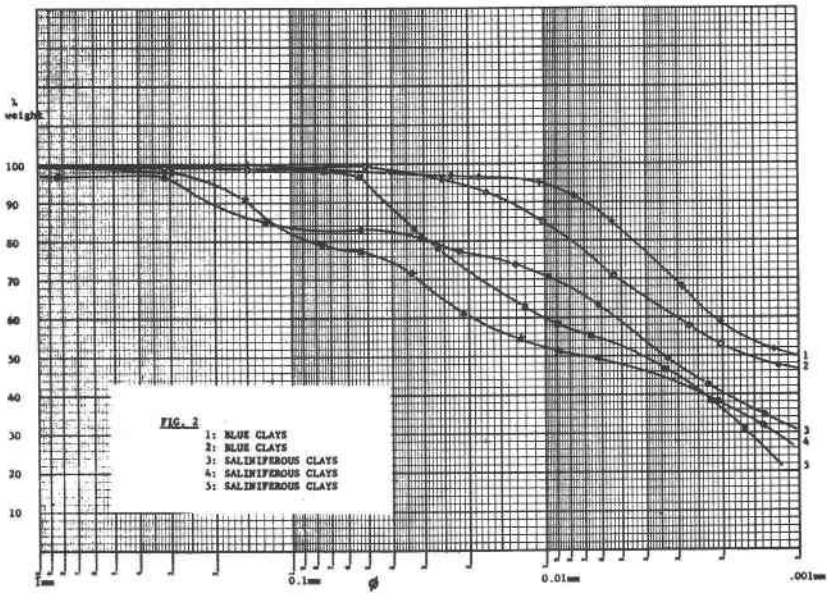

FIG. 2. Particle size distribution of the Willard clays.

tures lies in the weak bonds between interlayer cations and basal oxygens of layer silicates. The effect of the weathering should therefore be observable in the changes of the c dimension of the layers, which is determined in mica-type clay minerals by the interlayer forces. The elements of the interlayer forces are the electrostatic potential originating from the dissatisfied layer charges, the interlayer cations, and the permanent H_2O dipoles. Depending upon the decrease in layer charge, the mica-type clay minerals may be divided into several subgroups (Table 2).

The higher layer charges of the micas result in strongly bound interlayer cations and a constant interlayer separation. By the absence of layer charges, as in pyrophyllite, the interlayer separation also does not change. It is at the intermediate layer charges, as in vermiculites and mont-

morillonites, that variations in the interlayer separation occur. Illites possess a high layer charge which is partly satisfied by the inherent interlayer cations. Therefore, they show small amounts of unsatisfied charges giving rise to small variations of the interlayer separation.

The most important structural element in the interlayer region is the water molecule with its abnormal properties. The individual water molecule has a tetrahedral charge distribution. Under ordinary conditions the arrangement of the water molecules is similar to the arrangement of SiO_4 tetrahedra in quartz (Wells, 1952). Naturally, in liquid state the regularity is possible only over small regions and is continually being rearranged. When inserted into the electrical field of the interlayer region the H_2O tetrahedra will most likely extend the surface pattern of SiO_4

TABLE 2. LAYER CHARGE AND MICA-TYPE SUBGROUPS

	Layer charge per unit cell	Cation exchange capacity m.e./100 gm.	Equivalent of cation M exchange capacity per unit cell (unsatisfied charges)
Mica	0	0	0
Illite	1.3–1.5	1.–40	0.1–0.3
Vermiculite	1.0–1.3	100–150	0.8–1.3
Montmorillonite	0.3–1.0	67–100	0.5–0.8
Pyrophyllite	0	0	0

The values of the layer charge per unit cell, cation exchange capacity, and its equivalent per unit cell for illite, vermiculite, and montmorillonite are from Marshall (1964). Mica and pyrophyllite are included with their theoretical layer charges.

tetrahedra, since the water molecules have to arrange themselves to the layer surface at the tetrahedral angles. It follows that the interlayer cations will occupy the tetrahedral, octahedral, or larger holes between the H_2O sheets depending on the coordination number of the cations. The regularity of the interlayer arrangements will depend on both the effective layer charge and the polarizing power of the interlayer cations (the ionic potential Z/r). Further, the number of water molecules (thus the number of water layers) may be less than the coordination number of the interlayer cation, as in hydrated salts (Wells, 1952), that is, if the cation is also partly surrounded by the O atoms of the layer surfaces. The number of H_2O molecules may be also greater than the coordination number of the interlayer cation if additional H_2O molecules are attached to the other water molecules.

It is clear that the interlayer arrangement will become similar to the

liquid-state arrangement of H_2O with decreasing effective layer charge and with decreasing ionic potential of the interlayer cations. Two mica-type clay layers will give the same basal spacings only when they have similar layer charges and similar interlayer cations, and are exposed to the same relative humidity of the atmosphere. In identification of these layers it is therefore desirable to insert a known interlayer cation by means of ion-exchange treatment. For this purpose, the cations Mg^{2+} and K^+ are especially useful. Because of its high ionic potential (+3.0) Mg^{2+} can form stable Mg^{2+}-$(H_2O)_n$ layers between the mica-type layers, provided the effective layer charges are high enough, as in vermiculite. Because of its size and low ionic potential (+0.75) the K^+ can form a stable interlayer bond between mica-type layers, again if the effective layer charges are as high as in vermiculites.

It is useful in the interpretation of the x-ray diffraction effects on clay minerals to point out the importance of the "disorder" in the layer structures. Using Dornberger-Schiff's (1956) nomenclature of OD structures (order-disorder structures), micas generally consist of a sequence of layers characterized by the regular succession of one of the following stacking vectors:

$$S_1 = 1/3\boldsymbol{a}_1 + 2/3\boldsymbol{a}_2 + \boldsymbol{e} = 1/3\boldsymbol{b} + \boldsymbol{e}$$
$$S_2 = -(1/3\boldsymbol{a}_1 + 2/3\boldsymbol{a}_2) + \boldsymbol{e} = -1/3\boldsymbol{b} + \boldsymbol{e}$$

where $\boldsymbol{a}_1$ and $\boldsymbol{a}_2$ = basic hexagonal translation vectors within the layer; $\boldsymbol{b}$ = the orthohexagonal translation vector; $\boldsymbol{e}$ = a vector perpendicular to $\boldsymbol{a}$ and $\boldsymbol{b}$.

The regular stacking sequence of the mica-type layers may be degenerated in clay structures in two forms:

(a) The stacking sequence loses its regular succession, so that the layers no longer have a periodicity along the c axis. They interact with the x-rays as two-dimentional diffraction gratings. (b) The insertion of groups of atoms between layers generally causes three-dimensional disorder in the layer structures.

If the inserted atoms follow the a-b surface patterns, the insertion will change only the $\boldsymbol{e}$ component of the above stacking vectors and the layer structures will show variations only in the basal spacings of the layers.

Both forms of the disorder will be indicated by "continuous scattering" accompanying the normal Bragg reflections on the x-ray diffraction diagrams. The (00l), (hk), and (hkl) reflections of the Willard clays are discussed in the following pages according to the above concepts.

The (00l) reflections and variations in spacing and intensity. Diagnostic criteria to distinguish between the clay minerals are obtained primarily from the (00l) reflections. Oriented clay flakes were prepared from the −1.5 micron fraction of untreated samples for this purpose. Separate por-

tions of this fraction were saturated with the cations K^+ and Mg^{2+}. Another portion of the same fraction was acid-leached with weak organic acid (5 per cent solution of monochloracetic acid) and later saturated with K^+ and M^{2+}. *X*-ray diffraction patterns were obtained using a Philips Norelco diffractometer (Ni filter, Cu radiation, scale factor 8, multiplier 1, time constant 4, 1°/min. scanning speed).

The following are the clay minerals in the blue and saliniferous clays of the Willard Reservoir:

Illite: Illite is one of the main components, present both in blue and saliniferous clays, with characteristic reflections at 10.0, 5.0, 3.34 and 1.99 Å. In the blue clays, the 10.0 Å reflection displays an appreciable asymmetry. The intensity of the 10.0 Å reflection is decreased and its shape is improved (becomes more symmetrical) by glycerol treatment, especially by Mg^{2+} treatment and subsequent glycerol saturation (Fig. 3). In the saliniferous clays there is a pronounced continuous scattering between 10 and 14 Å (Fig. 4), indicating an intensive mixed layering between the mica-type layers with different spacings. This diffuse scattering cannot be attributed to the line-broadening effect of the particle size, because in the blue clays and saliniferous clays we examine essentially the same material and in the same particle size fraction. The situation can be visualized as a random intercalation of different cation-water layers between the basic 10 Å mica layers:

M
M
A = cation-H_2O layers
M
B = cation-H_2O layers · · ·

Thus the spacings of the MA, MB, · · · , composite layers will be different depending on the interlayer cations. A statistical mixing of these composite layers like MMAMBMCMA · · · will show on the *x*-ray diffraction diagrams apparent reflections whose spacings hold the following relation (Friedel, 1926):

$$d_{ap} = \gamma_M d_M + \gamma_{MA} d_{MA} + \gamma_{MB} d_{MB} + \gamma_{MC} d_{MC} + \cdots .$$

γ = proportion of one type composite layers, $\gamma_{MA} + \gamma_{MB} + \cdots = 1$. d_{ap} = apparent "intermediate spacing."

The continuous scattering between 10 and 14 Å in the Willard saliniferous clay minerals indicates a statistical stacking sequence of the M, MA, MB type layers. The distinguishable peaks superimposed on this continuous scattering at 10.6, 11.5, and 12.5 Å are the "intermediate spacings" and they indicate that there are different combinations of the M, MA, MB · · · type layers.

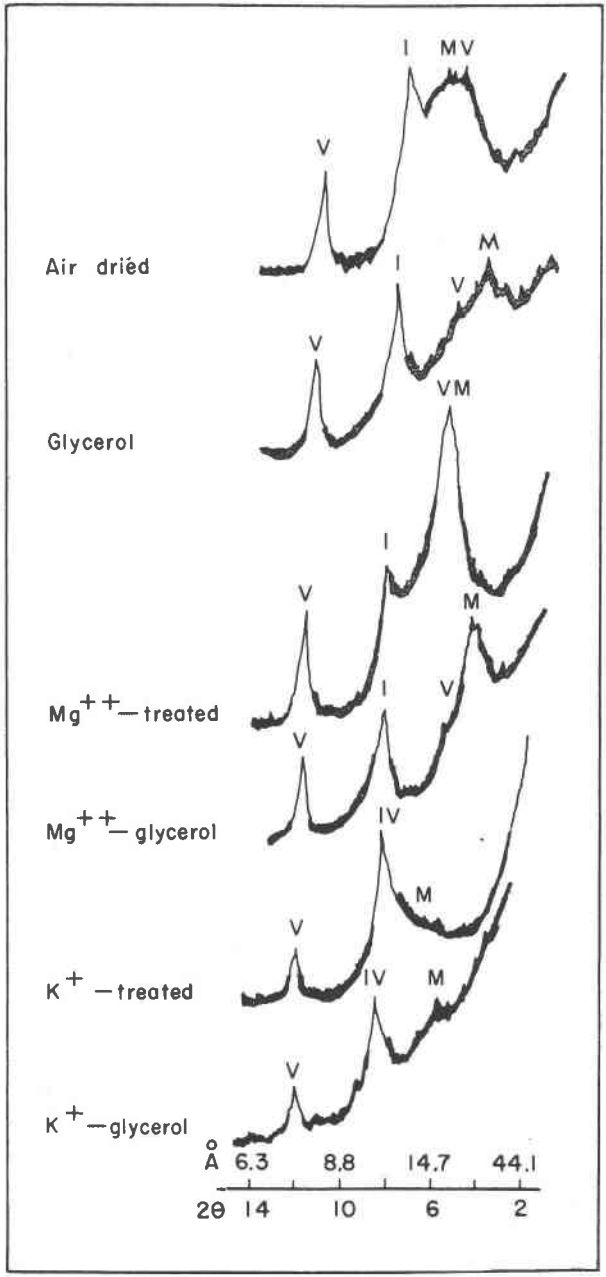

FIG. 3. *X*-ray diffraction patterns for oriented "blue clays" from Willard Reservoir (sample No. 1, minus 1.5 microns in natural state). I, illite; V, vermiculite; M, montmorillonite.

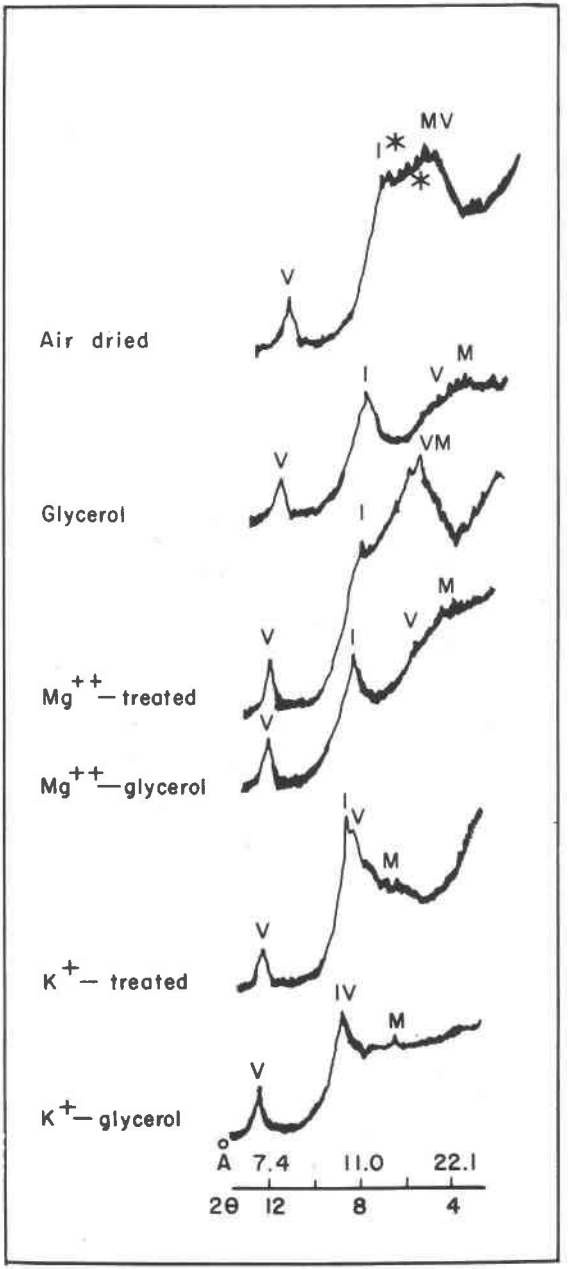

FIG. 4. *X*-ray diffraction patterns for oriented "saliniferous clays" from Willard Reservoir after acid treatment (sample No. 4, minus 1.5 microns fraction). I, illite; V, vermiculite; M, montmorillonite. Asterisk indicates intermediate spacings.

If the mixed layering is regular, like MMAMMA · · · , or MMBMMB · · · , or MAMBMAMBMAMB · · · , there will appear "superstructure" reflections (and possibly higher orders) with a spacing corresponding to d_M+d_{MA}, d_M+d_{MB}, or $d_{MA}+d_{MB}$ · · · . In the Willard clays the reflections between 20 and 30 Å are very weak and difficult to distinguish from the high background of the lower angle region.

Vermiculite: The observed reflections for vermiculite are 14.15 Å with a strong intensity; 7.13 Å, intensity medium; 4.7 Å, intensity weak; and 3.56 Å, intensity medium. Further, the reflections between 12.6 and 14.2 Å show several changes on heating at 110° C. for 1 hour and upon exposure to air; the 12.6 to 14.2 Å reflection band with a strong intensity is replaced by weak reflections at 14.3 and 11.6 Å; the 10.6 Å reflection of illite is highly increased in intensity. Upon increasing the temperature to 250° and 350° C. there is a further increase in intensity of the 10 Å reflection. Upon exposure to air, weak reflections appear between 10 and 15 Å which are caused by the sudden rehydration of vermiculite (Walker, 1961). At 450° C. all the reflections of 12.6 to 14.2 Å and the lower orders disappear and those of illite are highly increased in intensity. This heat treatment shows clearly that no chlorite is present.

The differentiation between vermiculite and montmorillonite is made by Mg^{2+} and K^+ saturation of the clay fraction in 1 N chloride solutions at 80° to 90° C. for 6 hours. In blue and saliniferous clays the 14.0 Å reflection of the Mg^{2+} clays so obtained gives rise, following glycerol saturation, to 18.2 to 18.9 Å and to 14.4 Å reflections (Figs. 3 and 4). The 14.4 Å reflection belongs, uniquely, to Mg vermiculite (Walker, 1961), whereas the expanded 18 to 19 Å layers correspond to montmorillonite.

In the blue clays the K^+ treatment causes contraction of the 14.2 Å reflection to 10.0 Å but leaves weak reflections at 10.8 and 14.3 Å. The 10.0 Å contraction indicates the presence of mica-type layers with a higher layer charge (vermiculite and illite). The weak reflections between 10.8 and 14.3 Å show, on the other hand, the presence of mica-type layers with lower layer charges (montmorillonite). In the saliniferous clays K^+ fixation causes the contraction of the 14 Å reflection to 10.3 Å, although leaving reflections at 11.15 Å and 12.6 Å. The 11.15 Å reflection probably belongs to the apparent intermediate spacings caused by the mixed layering between 10.3 Å layers and montmorillonite. The 12.6 Å reflection belongs most likely to montmorillonite (Fig. 4). The contraction of the K^+ saturated vermiculites toward 10 Å and the stable 14 Å reflection of the Mg^{2+} treated vermiculites are accounted for by the higher layer charges of these mica-type layers. Expansion of the Mg^{2+} montmorillonite to 18 to 19 Å and the partial concentration of the K^+ treated montmoril-

lonite to 12 Å is directly related to the lower layer charges of these mica-type layers. The amount of 0.7 negative charge per unit cell is generally accepted as the arbitrary boundary between vermiculite and montmorillonite (MacEwan, 1961).

Montmorillonite: The basal reflections of montmorillonite are not clearly shown in the *x*-ray diffraction patterns of the air-dried clay in its natural state. The 12.6 Å reflection in the natural state of blue clays indicates possible montmorillonite with monovalent interlayer cations. However, the Mg^{2+} and K^{+} treatment and glycerol saturation show clearly the presence of montmorillonite, as described above. In the saliniferous clay, montmorillonite is revealed after glycerol treatment of the acid-leached samples, with a reflection at 17.5 Å. Further, the glycerol saturation of Mg^{2+}-treated clay gives rise to reflections at 18 to 19 Å and K^{+} treatment causes contraction to 12.6 Å (Fig. 4).

The (hk) reflections and the b dimensions of the layers. An approximate relation between *b* dimensions and the composition of the layers has been shown by Veitch and Radoslovich (1963) in the form of a multiple regression analysis, under the assumption that the anion radii are constant.

Thus,

$$b = b_0 + \Sigma b_j x_j,$$

where b_0 = the *b* dimensions of the end member with the smallest dimensions; b_j = regression coefficient of the cation; and x_f = ionic proportion of the cation. In order to obtain the *b* dimensions of Willard clays, a focusing Guinier camera was used. This camera has a two-fold advantage: (a) oriented clay flakes can be mounted on the periphery of the camera, making it possible to obtain enhanced (*hk*) reflections from the clay flakes; (*b*) the high resolution of this camera makes it possible to differentiate between closely spaced lines. Table 3 gives the (*hk*) reflections of the Willard clays in the natural state and also after various forms of treatment.

The striking feature of the Guinier photographs is the presence of a continuous scattering accompanying the (02, 11) diffraction band. This fairly pronounced continuous scattering, which decreases toward higher angles, shows that the mica-type layers of the Willard clays have disorder in their stacking sequences. Because of this irregular stacking sequence the layers will interact with the *x*-rays as two-dimensional diffraction gratings, as indicated by the indices (*hk*). The displacements of the layers on each other are given by the $\pm nb/3$ components of the stacking vectors ($\mathbf{S}_1$, $\mathbf{S}_2$). The irregular stacking sequence does not affect the (0*k*0) reflections with $k = 3n$. The *b* dimensions of the layers have therefore been calculated from the 060 reflections. The *b* dimensions of the blue

TABLE 3. THE (*hk*) REFLECTIONS OF THE WILLARD CLAYS

	$d_{(hk)}$, Å	Indices (orthohexagonal)		
		(hk)	I	*b*, Å
		Sample No. 1, blue clay		
Untreated	4.47	02, 11	VS	
	2.57	20, 13	MW	
	1.501	060, 330	MW	9.01±0.01
Acid treated	4.47	02, 11	VS	
	2.58	20, 13	S	
	2.25	04, 22	VW	
	1.504	060, 330	M	9.02±0.01
	1.30	40, 26	VW	
Mg^{2+} treated	4.49	02, 11	VS	
	2.57	20, 13	MS	
	1.501	060, 330	MW	9.01±0.01
K^{+} treated	4.47	02, 11	VS	
	2.58	20, 13	M	
	1.504	060, 330	M	9.01±0.01
	1.30	40, 26	VW	
		Sample No. 4, saliniferous clay		
Untreated	4.49	02, 11	VS	
	2.58	20, 13	W	
	1.506	060, 330	VW	9.04±0.01
Acid treated	4.50	02, 11	VS	
	2.58	20, 13	S	
	1.507	060, 330	VW	9.04±0.01
	1.30	40, 26	M	
Mg^{2+} treated	4.50	02, 11	VS	
	2.58	20, 13	W	
	1.504	060, 330	S	9.02±0.01
	1.30	40, 26	M	

clays are 9.01 to 9.02±0.01 Å and those of the saliniferous clays 9.02 to 9.04±0.01 Å (the quartz lines being used as an internal standard). The *b* dimensions indicate clearly that all the layers are dioctahedral; and the *b* dimensions of the illites, vermiculites, and montmorillonites are the same. The *b* dimensions do not show any changes upon treatment with Mg^{2+} and K^{+} ions or after leaching with an organic acid. As seen in Table 3, there is an appreciable displacement of the maximum intensity of the (02, 11) diffraction band toward the higher angles. The spacing

TABLE 4. CHEMICAL ANALYSIS[1] OF WILLARD BLUE CLAY (−1.5 MICRON FRACTION)

Sample No. 1, Weight Per Cent

SiO_2	50.39
Al_2O_3	20.27
Fe_2O_3	6.96
FeO	1.31
TiO_2	0.43
MgO	3.83
CaO	0.71
K_2O	2.78
Na_2O	0.99
CO_2	1.06
P_2O_6	0.33
H_2O^+	10.96
	100.10

[1] Analyst, Silve Kallman, Ledoux and Company, Inc., New Jersey.

value of this diffraction band is lower than the calculated value from the (060, 330) reflections. The displacement of the maximum intensity of this diffraction band is also observed by Brindley and Robinson (1948) in metahalloysite and is related to the finite size of layers, as explained by these authors.

The (hkl) reflections and the polytypism of the layers. In order to obtain the (*hkl*) reflections, *x*-ray diffraction patterns from the *randomly oriented* samples of the Willard clays (less than 1.5 micron fraction) were taken. The *x*-ray diffraction pattern shows that the (*hkl*) reflections are absent in the blue clays and in the saliniferous clays. Except for the basal 3.33 Å reflection, which is enhanced by the presence of quartz, the two strong reflections at 4.47 and 2.57 Å are the two-dimensional (*hk*) reflections as described in Guinier photos. The absence of the three-dimensional (*hkl*) reflections indicates that the mica-type layers form a random stacking sequence in both Willard clays.

CHEMICAL ANALYSIS

A chemical analysis of one sample was obtained to provide additional information on the composite layer structure. To avoid the uncertainties concerning the salines and contaminants such as Fe-hydroxides and exchangeable cations, the sample was leached with a weak organic acid (5 per cent solution of monochloracetic acid), and the fraction under 1.5 microns was separated for analysis. The results of the chemical analysis are given in Table 4.

After subtraction for the small amount of quartz, feldspar, apatite, and dolomite, the remaining elements were used for the calculation of the formulae of the clay minerals of Willard Reservoir (No. 1). Since the clay minerals of this sample as shown by x-ray data are illite, montmorillonite, and vermiculite, the calculation of the formulae for the separate phases must be based on certain assumptions.

The ideal dioctahedral mica formulae are assumed for the mica-type non-expandable layers. All Na_2O and K_2O (as the clays are acid-leached) have been included in these formulae, and the corresponding amounts of SiO_2, Al_2O_3, MgO, and H_2O have been calculated. With the rest of the cations the composition of the expandable layers has been calculated without distinguishing between montmorillonite and vermiculite.

The second formula of the expandable layers has been calculated on the basis of 44 anionic valencies for the unit cell of the mica-type layers, as devised by Marshall (1949) and modified by Foster (1959).

Using the assumed mica formulae:

$$[Al_2(Si_3^{-1.0}Al)O_{10}(OH)_2]^{-1.0}(K, Na)_{1.0}^{+1.0}$$

and

$$[(Al_{1.64}Mg_{0.36})(Si_{3.26}Al_{0.74})O_{10}(OH)_2]^{-1.0}(K, Na)_{1.0}^{+1.0}$$

the calculated composition of the expandable layers becomes:

$$[(Si_{3.88}^{-0.12}Al_{0.12})Al_{0.76}Fe_{0.72}^{3+}Ti_{0.045}^{-0.43}Mg_{0.32}Fe_{0.165}^{2+})O_{10}(OH)_2]^{-0.56+0.56}R_{(\text{exchangeable})}$$

$$R^{3+}/R^{2+} = 1.53:0.49$$

and

$$[(Si_{3.73}Al_{0.27}^{-0.27})(Al_{1.03}Ti_{0.04}Fe_{0.70}^{3+}Fe_{0.15}^{2+}Mg_{0.31})O_{10}(OH)_2]^{-0.69+0.69}R_{(\text{exchangeable})}$$

$$R^{3+}/R^{2+} = 1.77:0.46$$

The b dimensions corresponding to the above formulae of the expandable layers are $b = 8.94$ Å and $b = 9.07$ Å, respectively, as calculated by the regression relations (Veitch and Radoslovich, 1963). Comparing these b values with the observed value $b = 9.02$ Å, it appears that the real composition of the expandable layers is probably intermediate between the given formulae. However, in both formulae for the expandable layers, the R^{3+}/R^{2+} ratios of the octahedra correspond to the dioctahedral occupation of the layers.

Discussion and Conclusions

The weathering sequence of the mica-type layer silicates is generally given in the following form: Mica (primary or secondary)→illite→vermiculite→montmorillonite. This weathering sequence is generally related to

a gradual K^+ depletion of the layers caused by decreasing layer charges. Substitution schemes like:

$$Fe^{2+}K^+ \rightarrow Fe^{3+}$$
$$Al^{3+}K^+ \rightarrow Si^{4+}$$

have been proposed to explain the above weathering sequence. There is no doubt that such substitutions occur in the layer silicates, but all these ion-per-ion substitution schemes are actually self-neutralizing, and therefore no variations in the effective charges on the surfaces of the layers can result.

Experiments by Correns (1963) on the artificial weathering of the silicates in open systems at low temperature (22° to 42° C.) similar to natural weathering provide useful information on the chemical decomposition of the silicates. From his results we may, for instance, calculate the ratio of the cations lost from the most stable layer silicate (muscovite powder of less than 1 micron) during artificial weathering under different *p*H conditions, as follows:

Ratio of cations lost per formula unit	*p*H=3	*p*H=5.8	*p*H=8.5	*p*H=11
$K^+:Al^{3+}:Si^{4+}$	0.45:0.12:0.25	0.7:0.05:0.4	0.6:0.1:0.2	0.66:0.1:0.2

Considering the original ratio of cations in the layer structure, $K^+:Al^{3+}:Si^{4+}=1:3:3$, the K^+ depletion corresponds to removal of minor amounts of Al^{3+} and Si^{4+} from the structure. Thus, micas will have some statistically unoccupied octahedral (Al^{3+}) and tetrahedral (Si^{4+} and Al^{3+}) positions with largely unsatisfied interlayer cationic positions. For instance, under mildly alkaline conditions (*p*H=8.5) the ratio of the lost cations will be $K^+:Al^{3+}:Si^{4+}=0.18:0.03:0.06$ or 6:1:2. Actually, Si values will be even lower, as part of the SiO_2 is also lost by the dissolution of the experimental material containing silica. The interlayer region will then be favorable for the insertion of groups of atoms because of unsatisfied charges. The few unoccupied sites in the layer will cause defects in structure or possibly will be occupied by other suitable cations (Fe, Mg). K^+ is then partly removed, and mica-type layers with dissatisfied layer charges are formed. There will be, of course, no strict boundaries between this stage of weathering and the following stage, but it is useful to adopt this view for the sake of simplicity.

Thus layer silicates that were similarly affected—as explained above—during their previous deposition and during their transport, which further reduces the grain size, will be accumulated in the Willard Reservoir. Now they may be regarded as colloidal particles with negative

surface charges in solution with mixed cations, mainly Na^+ and Ca^{2+}, as seen from saline minerals. The thermodynamics will require that the electrochemical potential of an ion must be the same everywhere in the system, as discussed in detail by Marshall (1964). We consider two points, X close to the charged surface and Y away from it, with ψ' and ψ'' the electrostatic potentials at these points, respectively. If the chemical potentials of the different ions (Na^+ and Ca^{2+} in this case) are given by $\mu_{(Na)X}$, $\mu_{(Na)Y}$, $\mu_{(Ca)X}$, $\mu_{(Ca)Y}$. At the points X and Y, respectively

$$\mu_{(Na)X} + z_1F\psi' = \mu_{(Na)Y} + z_1F\psi'' \qquad z_1 = 1, \text{ the valency of the ion}$$
$$\mu_{(Ca)X} + z_2F\psi' = \mu_{(Ca)Y} + z_2F\psi'' \qquad z_2 = 2$$

At constant temperature $\mu = RT \ln a + \mu^* \; a = \text{activity of the ion}$

$$RT \ln \frac{a_{(Na)X}}{a_{(Na)Y}} = \frac{1}{2} RT \ln \frac{a_{(Ca)X}}{a_{(Ca)Y}}$$

Replacing X by the clay surface and Y by the solution:

$$\left(\frac{a_{Na}}{\sqrt{a_{Ca}}}\right)_{\text{clay surface}} = \left(\frac{a_{Na}}{\sqrt{a_{Ca}}}\right)_{\text{solution}}$$

Activities can be written in terms of concentrations (c) and activity coefficients (f). Disregarding the changes in activity coefficients

$$(a_{Na}/\sqrt{a_{Ca}})_{\text{clay surface}} = (c_{Na}/\sqrt{c_{Ca}})_{\text{solution}}.$$

Thus the ratio of the cations Na^+ and Ca^{2+} near the clay surface depends on the concentration of these cations in the outer solution. As the saline content is low, the activity of Ca^{2+} is much higher and clay takes more Ca and less Na; but as the evaporation goes further the ratio $(a_{Na}/\sqrt{a_{Ca}})_{\text{clay}}$ increases and clay takes more Na and less Ca. Now if the charge distribution of the colloidal particles is homogeneous, in equilibrium similar (Na-Ca)-water layers will be formed on the surfaces of the particles. Thus in the stacking sequence MAMBMC $\cdots$ A, B, C would be equivalent layers and consisting of both cations in the thermodynamically given ratios. The blue clays which are permanently in contact with the saline water would be close to the equilibrium with the solution whose concentration is highly increased in Na. The broad x-ray diffraction band between 12.6 and 14 Å possibly indicates that the charge distribution of the layers is not homogeneous. The saliniferous clays which are dried with the precipitated salines will be heterogeneous in the distribution of both the cations and the layer charges, as is displayed by the "continuous scattering."

The expandable mica-type layers, vermiculite and montmorillonite, both being dioctahedral, have the same b dimensions, indicating that the layer compositions are similar to those of the illites present. Further, they

form a random mixed-layering with the illites which is the result of the changing layer charges and heterogeneous distributions of the interlayer cations. The expandable layers are therefore most likely the weathering products of the mica-type 10 Å layers.

The existence of expandable layers is important in determining the physical properties of this material. The clay minerals with susceptible interlayers are likely to be very sensitive to environmental changes. They show sudden contraction upon dehydration and expansion upon rehydration, caused by changes of temperature and humidity.

The values of the *b* dimensions show that the layer structures of the Willard clays have a dioctahedral occupation. The chemical analysis shows low Al_2O_3 content and high SiO_2 content for a muscovite mica; although weathering would slightly decrease the SiO_2/Al_2O_3 ratio in the layer silicates as shown above. Further, the appreciable amounts of $MgO+FeO+Fe_2O_3$ cannot be expected from a muscovite-type mica, nor can they be explained by filling the available Si, Al positions during the weathering of the layers. The values of the *b* dimensions and the results of the chemical analysis indicate the tetrasilicic nature of the mica-type layers before the weathering.

Acknowledgments

This study has been made possible by a Columbia University Boese post-doctorate fellowship and the support of the U. S. Air Force Cambridge Research Laboratories. The Guinier films were taken in the *x*-ray laboratory of the Brooklyn Polytechnical Institute, where we much appreciate the interest shown by Dr. Judith Bregman, Associate Professor in the Physics Department. We thank Dr. T. P. Rooney and Mr. H. D. Needham of Columbia University for their interest and assistance. We thank Dr. C. W. Burnham of the Geophysical Laboratory for reading the manuscript and for his constructive suggestions.

References

Brindley, G. W. and K. Robinson (1948) *X*-ray studies of halloysite and metahalloysite, Part I. *Mineral. Mag.* **28,** 393–406.

Correns, C. W. (1963) Experiments on the decomposition of silicates and discussion of chemical weathering. *Proc. 10th Natl. Conf. Clays and Clay Minerals,* 443.

Dornberger-Schiff, K. (1956) On order-disorder structures (OD-structures). *Acta Cryst.* **9,** 593–601.

Foster, M. D. (1959) Interpretation of the composition of trioctahedral micas. *U. S. Geol. Survey Prof. Paper* **354-B,** 11–49.

Friedel, G. (1926) *Lecons de Cristallographie,* Berger-Levrault, Paris, p. 395.

MacEwan, D. M. C. (1961) Montmorillonite minerals. In, *The X-ray Identification and Crystal Structures of Clay Minerals,* Mineral. Soc., Clay Minerals Group, London, p. 143–207.

MARSHALL, C. E. (1949) *The Colloid Chemistry of the Silicate Minerals*, Academic Press, New York, p. 195.

——— (1964) *The Physical Chemistry and Mineralogy of Soils, Vol. 1, Soil Materials*, John Wiley & Sons, Inc., New York, p. 113–121.

VEITCH, L. G. AND E. W. RADOSLOVICH (1963) The cell dimensions and symmetry of layer lattice silicates, III, Octahedral ordering. *Am. Mineral.* **48**, 62–75.

WALKER, G. F. (1961) Vermiculite minerals. In *The X-ray Identification and Crystal Structures of Clay Minerals*, Mineral. Soc., Clay Minerals Group, London, p. 297–324.

WELLS, A. F. (1952) *Structural Inorganic Chemistry*, 2d edition. Clarendon Press, Oxford, p. 427–449.

Manuscript received, February 23, 1965; accepted for publication, April 1, 1966